

Plasmonic Terahertz Wave Detector Based on Silicon Field-Effect Transistors with Asymmetric Source and Drain Structures

Min Woo Ryu¹, Kibog Park¹, Wook-Ki Park², Seong-Tae Han² and Kyung Rok Kim^{1*}

¹Ulsan National Institute of Science and Technology (UNIST), Ulsan 689-798, South Korea

Phone: 82-52-217-2177, Fax: 82-52-217-2109, *Email: krkim@unist.ac.kr

²Korea Electrotechnology Research Institute, Ansan, Gyeonggi 426-910, South Korea

Since terahertz (THz) wave detection mechanism by using oscillations of channel plasma waves based on a field-effect transistor (FET) structure was proposed by Dyakonov and Shur [1], FETs with 2-dimensional electron gas (2DEG) in the channel have been intensively investigated as the promising plasmonic detectors of THz radiations. In this letter, we report the experimental demonstrations of the enhanced responsivity in Si metal-oxide-semiconductor (MOS) FET-based plasmonic THz detector [2, 3] with asymmetric source and drain region considering the device width variations.

The devices with $L_g = 2 \mu\text{m}$, and $t_{\text{ox}} = 50 \text{ nm}$ were fabricated on the $1 \times 10^{15} \text{ cm}^{-3}$ p-doped <100> Si wafer. The threshold voltage (V_{th}) extracted from the transfer characteristics at low drain bias was within the range of $V_{\text{th}} = 0.2 \sim 0.6 \text{ V}$ for all devices (see Fig. 1). Figure 2 shows the measurement setup with lock-in amplifier system for the responsivity of the fabricated plasmonic THz detector. The sub-THz radiation with frequency $f = 0.2 \text{ THz}$ was generated by a gyrotron source in higher order mode resonator, which enables real-time detection with the continuous-wave (CW) method since it is stable in sub-THz frequency regime [4]. Figure 3 shows the image of the detector contact pads on the wafer sample with bonding wires. It should be noted that these bonding wires also can act as antennas by exposing directly to THz wave since the wire length is longer than the half of the wavelength ($\lambda/2 = f/2c = 0.75 \text{ mm}$ at $f = 0.2 \text{ THz}$) [3, 5]. Figure 4 presents the micrograph image (top view) of the fabricated Si FET with asymmetric source and drain structure. Asymmetric structure condition is determined by split of the source width W_s as $2 \mu\text{m}$, $10 \mu\text{m}$, $15 \mu\text{m}$, and $20 \mu\text{m}$ with the fixed drain width $W_D = 20 \mu\text{m}$. The corresponding asymmetry ratio $\eta_a (= W_D/W_s)$ would be 10, 2, 4/3, and 1 respectively.

As shown in Fig. 5, the peak values of the measured Δu to 0.2 THz radiation near threshold increase as the electric current of the gyrotron source grows from 70 to 100 mA. It should be noted that these response signals totally result from the gyrotron THz source since there is no response signal when the current is 0 A. The emission power at the end of waveguide has been estimated as 10 W by using the calorimeter when the electric current in our gyrotron source is 80 mA (default) and the actual power to be delivered onto the detector may be reduced by considering the device dimension and diffraction limit. In Fig. 6, we obtained the reproducible photoresponse for various detectors (T1~T4) with different asymmetry ratio ($\eta_a = 10$ for T1 and T2, $\eta_a = 4/3$ for T3 and T4) and more enhanced responsivity for the detectors with larger asymmetry ratio (T1, T2 with $\eta_a = 10$). The responsivity in this plot of Fig. 6 has been normalized by the maximum value (T1, T2) with arbitrary unit in order to confirm the relative photoresponse results for the different asymmetry ratio. In our proposed asymmetric structure, these asymmetric boundary conditions internally arise by the difference of the gate overlap capacitances between source and drain and thus, the responsivity R_V starts to appear and increases as the structural asymmetry between source and drain area under the gate increases. To find the maximum R_V at their own antenna coupling effects for each asymmetry ratio η_a , the detector sample holder is rotated from 0° to 360° step-wise with 30° (12 steps) in the transverse plane of the polarized THz wave propagation, because the orientation of the bonding wires has significant effect on the response signal to the polarized THz radiation [5]. Figure 7 shows the normalized experimental data R_V versus detector sample rotation angle and indicates that the peak R_V occurs at the different rotation angle (210° for T1 with $\eta_a = 10$ and 0° for T3 with $\eta_a = 4/3$) that is aligned with gate bonding wires to the polarized radiation. By considering these orientation effects with the bonding wires on the photoresponse, we obtained the more enhanced R_V about 5 times as η_a increases from 4/3 to 10, while the response signal in the symmetric detector (square) is negligibly small as shown in Fig. 8. At the same initial angle of 0° , however, it was 2.4 times of R_V ratio between $\eta_a = 4/3$ and 10 (see Fig. 6).

In conclusion, we have experimentally demonstrated that the plasmonic THz detector based on Si FETs with asymmetric source and drain structures can enhance the responsivity at room temperature. These results can provide the possibility of the performance enhancement focusing on the asymmetric design of source and drain structure under the gate in field-effect devices without additional considerations of external antenna and amplifier integration.

Acknowledgements: This work was supported by the Joint Research Project of the Korea Research Council for Industrial Science and Technology (ISTK), Republic of Korea.

Refs.: [1] M. Dyakonov and M. Shur: Phys. Rev. Lett. **71**, 2465 (1993); M. Dyakonov and M. Shur: IEEE Trans. Electron Devices **43**, 380 (1996) [2] W. Knap et. al, Appl. Phys. Lett, **85**, 4 (2004) [3] R. Tauk et. al, Appl. Phys. Lett, **89**, 253511 (2006) [4] S. T. Han et. al, 2009 34th TRMMW-THz [5] M. Sakowicz et. al, Appl. Phys. Lett, **104**, 024519 (2008)

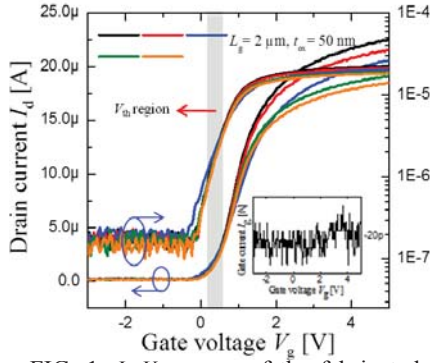


FIG. 1. I_d - V_g curves of the fabricated Si-FETs. The threshold voltage V_{th} extracted from these DC curves at $V_d = 1$ V. Inset shows the negligible gate current for all gate voltages.

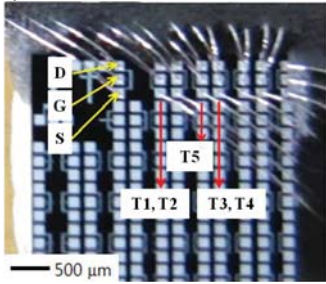


FIG. 3. Photo image of the detector sample with bonding wires on the sample board. ($\eta_a = 10$ for T1 and T2, $\eta_a = 4/3$ for T3 and T4, $\eta_a = 2$ for T5).

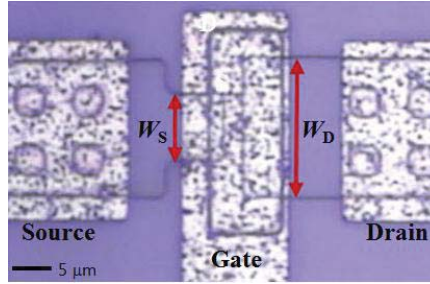


FIG. 4. Micrograph (top view) of the fabricated Si FET with asymmetric source and drain. Drain width $W_D = 20$ μm and source width $W_S = 2, 10, 15,$ and 20 μm with corresponding asymmetry ratio $\eta_a = W_D/W_S$ is 10 (T1, T2), 2 (T5), $4/3$ (T3, T4) and 1 (symmetric), respectively.

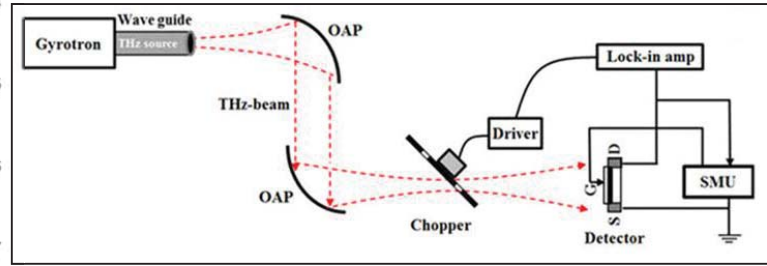


FIG. 2. Schematic of the experimental setup for plasmonic THz detector using 0.2 THz gyrotron source

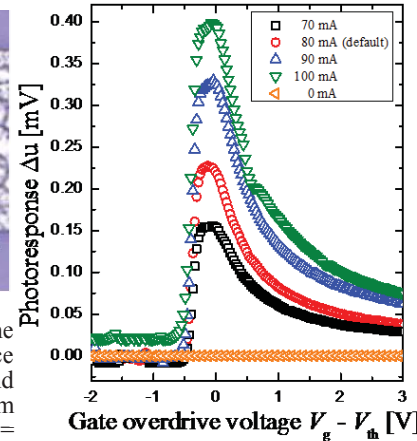


FIG. 5. Experimental results of the Si FET response signal to 0.2 THz radiation. Photoresponse Δu as a function of the gate overdrive voltage $V_g - V_{th}$ for different emission power by varying the current in gyrotron source.

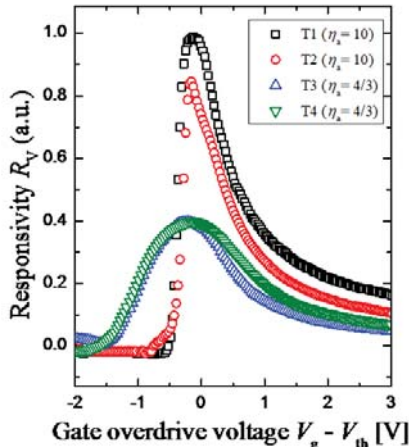


FIG. 6. Responsivity R_v as a function of $V_g - V_{th}$ for various Si FETs (T1, T2, T3, T4) with different values of the asymmetry ratio $\eta_a = 10, 4/3$.

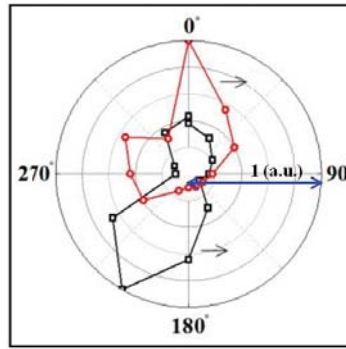


FIG. 7. The normalized amplitude of the response signal versus sample rotation angle. The detector sample holder is rotated from 0 to 360° step-wise with 30° in the transverse plane of THz ray.

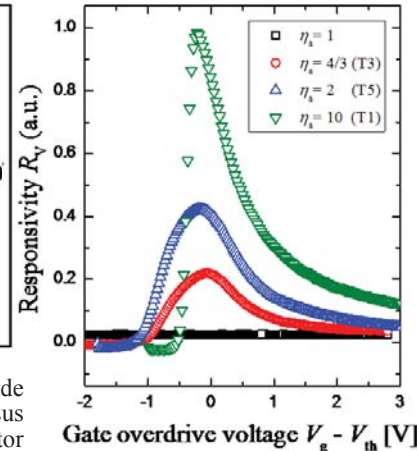


FIG. 8. Responsivity R_v as a function of $V_g - V_{th}$ for the different asymmetry ratio η_a are 10 (T1), 2 (T5), $4/3$ (T3), and 1 (symmetric).